Ink-particle Flight Simulation for Continuous Inkjet Type Printer

Masato Ikegawa[1], Eiji Ishii[1], Nobuhiro Harada[2] and Tsuneaki Takagishi[2]

[1]Hitachi Research Laboratory, Hitachi Ltd., Ibaraki, Japan
[2]Marking Systems and Hoist Systems Division, Hitachi Industrial Equipment Systems Co., Ltd., Ibaraki, Japan

Abstract

Industrial continuous inkjet printers typically are used for printing directly on various types of products such as cans, bottles, and food packaging in production lines. Their application to 3D printing (additive manufacturing) also has recently become a promising area of research. To enable their application to higher speed production lines, their print quality needs to be improved. This means that ink-particle flight simulation technology is needed to clarify the factors that affect print quality. Print distortion results from aerodynamic and electric interference among the ink-particles during their flight from the nozzle onto the print target. A simulation technique has been developed that enables the trajectories of the ink particles and the airflow around them to be calculated simultaneously. The functions needed to accomplish this, such as calculation of the electrostatic force, the Coulomb force, and the aerodynamic drag force for many flying ink particles were added to a Lagrangian method used for fluid dynamic analysis. The simulated velocities and positions of the flying ink particles agreed well with the experimental ones and helped clarify the factors affecting print quality. Simulated printing of multiple-dot lines revealed that the lines on the print target were distorted. This was because the trajectories of the charged particles in the lines were distorted by electric and aerodynamic interference during flight. Simulation showed that the appropriate insertion of dummy particles reduces the print distortion in computers.

Introduction

Since continuous inkjet printers (CIJPs) were originally devised by several inventors, i.e., Thomson [1], Sweet [2], and Herz and Simonsson [3], they have been improved for practical uses. Industrial CIJPs are used on many production lines for printing on various types of products such as cans, bottles, packages, and food packaging [4, 5] because the print distance can be set wider and the printing speed can be set faster than with drop-on-demand printers. Their application to 3D printing (additive manufacturing) is also now a promising area of study. To enable their application to higher speed production lines, the print quality needs to be improved. Therefore, ink-particle flight simulation technology is needed to clarify the factors that affect print quality, and algorithms are needed to reduce it.

Ink particles are formed by the breakup of an inkjet as it is ejected from a printer nozzle. The particles are charged between charging electrodes (charge electrodes) and are deflected between charged electrodes (deflection electrodes) so that they are directed toward the print target. Print distortion (difference between ideal position and printed one) occurs due to aerodynamic and electric interference between the particles during flight. Clarification of this distortion effect requires that the trajectories of the particles and the airflows around them are simultaneously calculated.

The mechanism for droplet formation in CIJPs was theoretically investigated by Rayleigh [6] and Weber [7], and it was recently simulated [8, 9]. The mechanism for drop charging and deflection was investigated by Suzuki and Asano [10] and Filmore et al. [11]. Droplet spreading on the target was investigated by Ikegawa and Azuma [12]. However, the airflow around ink particles has not been sufficiently clarified [13–15]. Watanabe et al. [15] used one-dimensional simulation with a simplified airflow model to represent the area around the ink particles to analyze their trajectories, which were compared with experimental results. Three-dimensional trajectory simulation is eagerly anticipated.

We have developed a simulation technique that solves these problems. The functions needed to accomplish this, such as calculating the electrostatic force in the electric field between the electrodes, the Coulomb force from other charged particles, and the drag force in the inkjet stream were added to a Lagrangian method used to analyze fluid dynamics [16]. With this technique, the trajectories of the ink particles and the airflow around them can be calculated simultaneously. The simulation agreed well with the experimental ones obtained with a high-speed camera.

Printing of multiple-dot lines was also simulated. The print lines were distorted because the trajectories of the charged particles were distorted by electric and aerodynamic interference during flight. This paper focuses on the print distortion of multiple-dot lines and its mechanism.

Numerical Simulation and Experimental Method

Problem Phenomena

The forces affecting flying ink particles are aerodynamic drag, electric force and Coulomb force. Here, electric force is the force that ink particles receive in a static electric field, and Coulomb force is the force that they receive from other charged ink particles. The factors that cause particle trajectory errors are aerodynamic interference and Coulomb force among particles.

Figure 1 is a schematic of the principles underlying a CIJP. An ink-supply pump (not shown) pressurizes the ink so that it flows through the nozzle. Ultrasonic vibration breaks the pressurized ink stream into small droplets. The droplets then fly sequentially with a certain interval from the nozzle toward the print target. Each droplet is selectively charged by charge electrodes that apply a signal that corresponds to the character to be printed. A high voltage is applied to the deflection electrodes. As the charged droplets pass between these electrodes, they are deflected by an

amount proportional to the charge. The charged droplets then reach the print target, which they hit sequentially from bottom to top. The target moves across the print head almost at right angles to the direction of the deflected droplets. In this manner, printed characters are formed as two-dimensional dot matrixes on the target. The non-charged droplets which are not used for printing are caught by a gutter and returned as ink to an ink bottle (not shown). The droplets are called "ink particles" here. An airflow is induced around them during flight. Print distortion occurs due to changes in their trajectories resulting from the aerodynamic and Coulomb interference between them.

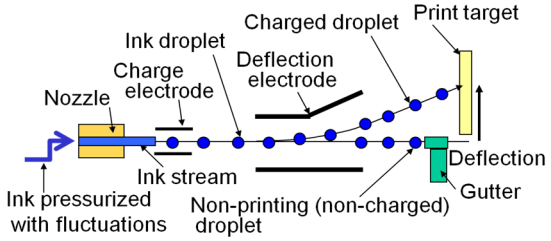

Figure 1 Schematic of principles for continuous inkjet printer

The distance between the ink particles at the beginning of breakup is almost equivalent to the wave length, λ, of the ultrasonic vibration. The relationship between wave-length λ and ink-particle diameter d_d is $\lambda = \sim 2.4\ d_d$. Therefore, trailing ink particles inevitably suffer aerodynamic interference in the wake of the leading ink particles and this reduces drag. The aerodynamic interference on the trailing particles decreases when the leading ink particles change their direction due to the electric force between the deflection electrodes.

Numerical analysis

The numerical analysis was done using three-dimensional fluid simulations with incompressible and isothermal conditions and the finite volume method under a conservative scheme were used. The governing equations, i.e., a continuity equation and the Navier-Stokes equation, are written as

$$\begin{cases} U_{i,i} = 0 & (1) \\ \dot{U}_i = -P_j / \rho + \nu (U_{i,j} + U_{j,i})_j & (2) \end{cases},$$

where U_i is the ith component of velocity, $U_{i,j}$ is the x_j directional derivative of U_i , and $\dot{U}$ is the time derivative of U. Here, P_j is the x_j directional derivative of pressure P, ρ is the density of air, and v is the kinematic viscosity of air. The subscripts used comply with the summation law.

As mentioned, the necessary functions, such as the calculation of the electrostatic force, the Coulomb force, and the aerodynamic drag force were added to a Lagrangian method used for fluid dynamic analysis [16]. The airflow and electric field were calculated using STAR-CD computational fluid dynamics software (v4.10) [17].

Almost 260 ink-particles were needed to predict characters in the simulation. It was impractical to build fine meshes around 260 ink particles and analyze them as an Eulerian two-phase flow because the large-scale calculations that need a long calculation time needed. A dispersed multi-phase flow model (Lagrangian model) was better for analyzing the flow as the dispersed phase of a continuous aspect of the vapor phase and the particles, and the trajectories of the ink particles were calculated as kinetics with outside forces while the airflow was analyzed under unsteady conditions. Unsteady flow was calculated by using the pressure implicit with splitting of operator (PISO) method with a fully implicit method.

The outside forces that an ink particle receives are Coulomb force F_{cl} from other charged ink particles, air drag F_{dr} from the surrounding air, and electric force F_{el} from the static electric field. In addition, small particles are generally subject to gravity, virtual mass force, and Basset force, but these effects are neglected here because they are very small under our simulation conditions.

Newton's equation of motion for a particle is

$$m_d \frac{dU_d}{dt} = F_{dr} + F_{el} + F_{cl} \quad , \quad (3)$$

where m_d is the mass of the particle, U_d is its velocity, and t is time.

Equation (3) is integrated with the first order of Euler's implicit method, and the momentum changes exchanged through the transported fluid in the cell through which the particle passes in the dispersed multi-phase flow (Lagrange model) method. The conversion rate of the entire mass and energy is similarly evaluated through integration and the sum total of the corresponding equation.

1) Air drag

Air drag F_{dr} can be written as follows using drag coefficient C_D:

$$F_{dr} = \frac{1}{2} C_D \rho A_d |U - U_d| (U - U_d) \quad , \quad (4)$$

where ρ is the density of air, A_d is the sectional area of the ink-particle, and U is the velocity of the surrounding air.

Ink particles were assumed to be spherical on the basis of measurements obtained from a photograph taken after such particles passed between the deflection electrodes. We used Beard and Pruppacher's empirical equation below for C_D [18].

$$\begin{aligned} C_D &= (24/\mathrm{Re}_d)(1 + 0.102\,\mathrm{Re}_d^{\,0.955}) \quad (0.2 < \mathrm{Re}_d < 2) \\ C_D &= (24/\mathrm{Re}_d)(1 + 0.115\,\mathrm{Re}_d^{\,0.802}) \quad (2 < \mathrm{Re}_d < 21) \\ C_D &= (24/\mathrm{Re}_d)(1 + 0.189\,\mathrm{Re}_d^{\,0.632}) \quad (21 < \mathrm{Re}_d < 200) \end{aligned} \quad , \quad (5)$$

where Re_d is the particle Reynolds number, which is defined as

$$\mathrm{Re}_d = \frac{|U - U_d| d_d}{\upsilon} \quad , \quad (6)$$

where v is the kinematic viscosity of air.

What needs special attention here depends on the expressions in Eqs. (4) and (5): F_{dr} is a function at a relative speed (U-U_d), and U in the surrounding airflow has an important effect. Lined ink particles draw peripheral air into the stream, thus generating a jet boundary layer, which greatly increases the velocity of the surrounding airflow.

Several groups have examined experimentally the drag coefficient of a trailing sphere [19–20]. Tsuji et al. plotted the relationship of the drag coefficient ratio between a trailing sphere and a single, C_D/C_{D0}, and interval L between the two spheres in a tandem arrangement [19]. The drag coefficient, C_D, of the trailing sphere decreases more than that C_{D0} of a single sphere when the L/diameter D_{sp} ratio is less than six. The empirical formula fitted with a second order approximation for Tsuji et al.'s experimental data was used in the subroutine used to calculate drag in the simulation of flying ink particles. Tsuji et al. also found that the

drag coefficient of the leading sphere was unaffected by the trailing sphere.

2) Electric force

The static electric field was analyzed with the STAR-CD software (version 4.10). Electric force F_{el} in Eq. 7 was applied to an ink particle with charge q in electric field E between the deflection electrodes.

$$F_{el} = qE \quad . \tag{7}$$

3) Coulomb force

Coulomb force F_{cl} on an ink particle is the sum of the Coulomb forces from all the other ink particles surrounding it. Therefore, all the ink particles surrounding the ink particle under examination (charge q) are identified, and the Coulomb forces from all the ink particles at distance r_i and with charge q_i are summed up :

$$F_{cl} = \sum \frac{1}{4\pi\varepsilon_0}\frac{qq_i}{r_i^2} \quad , \tag{8}$$

where ε_0=8.854E-12 [$A^2s^2N^{-1}m^{-2}$] is the permittivity of the vacuum electric constant.

4) Numerical model

The calculation area is the space from the inlet (nozzle exit) to the print target, as illustrated in Fig. 2. The ink particles fly along the *yz* plane as shown in the figure. The area for the calculations was enclosed by the charge electrodes, the deflection electrodes, the print target, and the atmospheric pressure boundaries. The direction of *x* was established to be 1.6 mm in width and symmetry boundaries were created for both walls.

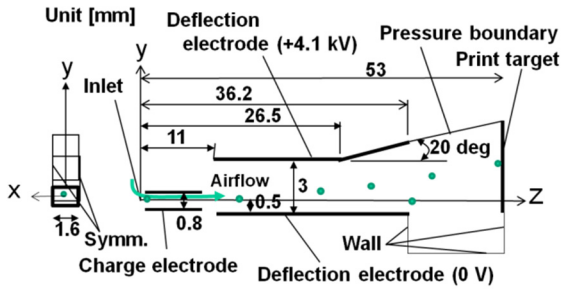

Figure 2 Definition of calculation area

The ink particles are sequentially discharged from the starting point (nozzle exit center) in the *z* direction at an initial speed and constant interval. They form an "ink beam", which passed along the center line between the charge electrodes and along a line 0.5 mm above the ground deflection electrode. The gutter into which non-charged ink particles entered was neglected in the simulation. The voltage of the positive deflection electrode was set to +4.1 kV, and that of the ground deflection electrode was set to 0 V.

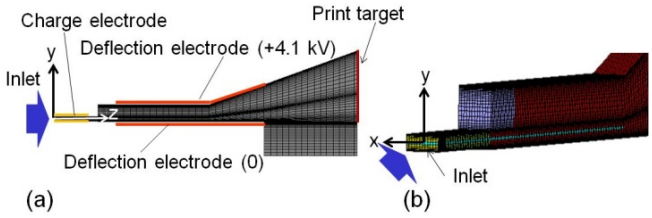

Figure 3 (a) Entire mesh chart (202,548 cells), and (b) mesh chart as viewed from inlet

The mesh (hexahedron) used for the STAR-CD analysis (shown in Fig. 3) had 202,548 cells. The first-order central difference method was used for calculating the space derivatives.

5) Calculation method

Since the Reynolds numbers for the airflow and the ink particles were respectively ~400 and ~200, the flow could be treated as a laminar flow. Therefore an unsteady airflow, a laminar airflow, and a two-phase flow (Lagrangian) were used.

The simulation code was verified by the experimental results for the change in velocities and trajectories for two flying ink particles with a certain interval. The simulated aerodynamic effects were first verified by the velocities of two non-charged ink particles, and then the simulated aerodynamic and electrical effects were verified by the trajectories of two charged ink particles flying between the deflection electrodes [16]. Since many more particles than two fly toward the print target, we investigated the effect of interferences among many particles on print quality here.

6) Multiple-dot printing

We investigated the printing of five lines with seven dots (each line was composed of seven particles). Table 1 lists the parameters of the ink particles used in the simulations and experiments. One case with an initial velocity, diameter, and initial particle interval was used in all simulations.

Table 1 Ink-particle parameters for simulations and experiments (nozzle diameter: 65 μm)

Initial ink-particle velocity w_{d0} [m/s]*	20.90
Density of ink-particle ρ_d [kg/m^3]	890.0
Diameter of ink-particle d_d [μm]*	125.0
Initial interval L_0 [μm]*	304.0

*Measured with high speed camera (Photron FASTCAM-APXRS; resolution: 256×256 pixels; frame rate: 30,000/s)

Table 2 shows the ink-particle charges for the five lines with seven dots. The charges for all lines were the same.

Table 2 Ink-particle charges of seven dots in each line

Dot no.	Charge [C]
1	-7.735 x10^{-13}
2	-9.203 x10^{-13}
3	-1.067 x10^{-12}
4	-1.213 x10^{-12}
5	-1.361 x10^{-12}
6	-1.508 x10^{-12}
7	-1.655 x10^{-12}

These analysis models were applied to an experimental CIJP (nozzle diameter of 65 μm). The experiments were conducted under the same conditions, and the positions of the ink particles were measured at three points in the z direction within the deflection electrodes using a high-speed camera (Photron FASTCAM-APXRS).

Results and Discussion

The ink-particle flight analysis was done by using the developed simulator, and the simulated print patterns on the print target were compared with the experimental ones.

Flight of ink particles

The printing simulation results were compared with the experimental ones. In the simulation, the charged particles for forming five lines with seven dots flew after 200 non-charged particles had flown. The particles were sequentially discharged from the nozzle along the *z* axis line at a constant interval. In the experiment, the non-charged particles flew continuously, and an airflow was formed before the flight of the charged particles. In the simulation, 200 non-charged particles flew first, and then the charged particles for forming five lines with seven dots flew. A previous report [16] showed that the airflow distribution reaches a steady state once 200 particles have flown, so the number of initial non-charged particles was set to 200.

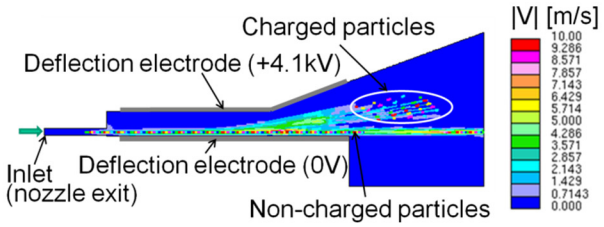

Figure 4 Velocity distribution and particle positions at 0.0020 s

The simulation results of the positions of the particles and the airflow velocity distribution at 0.0020 s after the first charged particle was discharged from the nozzle are shown in Fig. 4. A jet boundary layer was found to form around the flying particles.

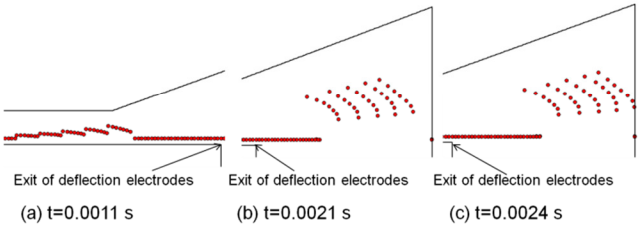

Figure 5 Positions of charged particles for five lines at three time points (simulation)

The positions of the charged particles at three time points in the simulation are shown in Fig. 5. Each line is standing up from the beam at around t = 0.0011 s. The intervals between lines are equal distance at this stage. At t = 0.0021 s, the interval between the first and second lines was narrower than the others, and the lines were curved. These cause the print distortion. At t = 0.0024 s, the lines of dots began to striking the target. The curvatures and inconsistent spacing caused print distortion.

Print results

The print results between the simulation (a) and experiment (b) are compared in Fig. 6. They show a good agreement. The print target ran in the x direction (perpendicular to the sheet in Fig. 5) at 400 m/min. The seven particles in the first (the leftmost) line are represented by the sequential dots from bottom to top, and the other four lines are similarly shown from left to right. The results of the particle positions revealed several print distortions.

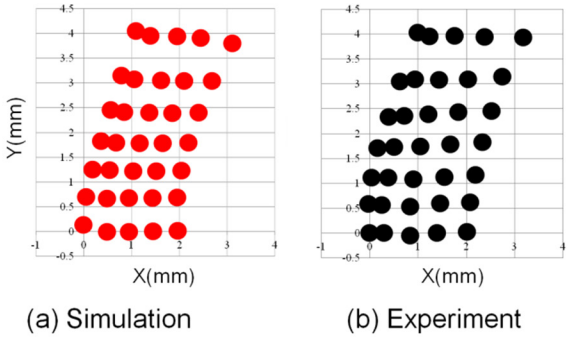

Figure 6 Print results: (a) simulation, (b) experiment

The lines were curved, the interval between the first and second lines was narrower than the others, and the top dots were shifted to the up and right.

Effect of air drag and Coulomb force

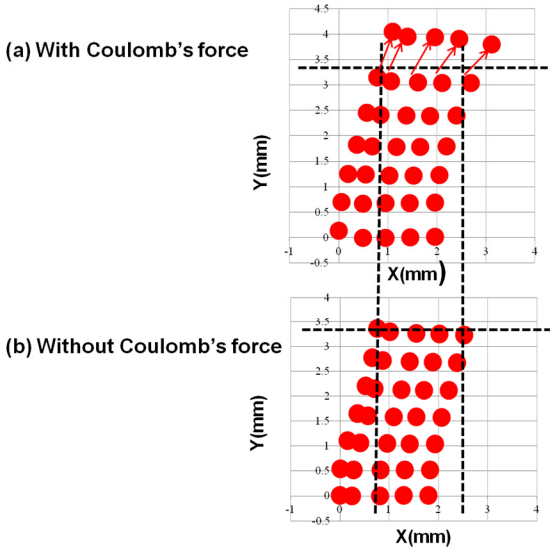

Figure 7 Effect of Coulomb repulsive force on print result (simulation) (a) with and (b) without Coulomb force

The simulation results with and without Coulomb repulsive force are compared in Fig. 7. The results without Coulomb force show the effect of air drag. We found that the effects of air drag on

print distortion were to narrower the first and second lines and curve the lines. The print distortion caused by Coulomb force shows reflects the lower speed of the seventh (top) dot, the wider interval between the sixth- and seventh dots, and the deceleration of the last particle.

Print distortion correction with dummy particles

The ideal print pattern is composed of diagonal parallel lines. This means that the lines can be printed in parallel with wider distances between charged particles. One of the techniques for it is the method of inserting dummy (non-charged) particles between the charged ones. Figure 8 shows that inserting non-charged dummy particles reduces print distortion by reducing the interferences caused by aerodynamic and Coulomb forces with an increase the distances between charged particles and lines.

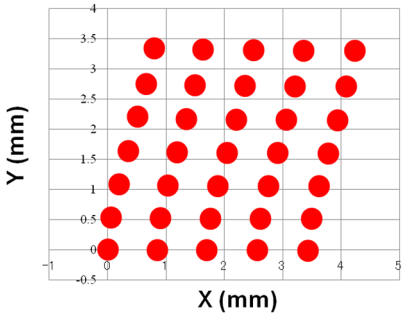

Figure 8 Effect of inserting dummy particles (simulation)

The correction was made by inserting four non-charged particles between lines, and two between dots. The speed of print target is 200 m/min. As a result, the lines can be made straight and parallel by appropriate insertion of dummy particles.

This simulation technique can thus be used to design CIJPs for decreasing print distortion in computers.

Conclusions

The flight of ink particles for forming multiple-dot lines in an industrial continuous inkjet printer was simulated on the basis of electric and aerodynamic physics. Commercial fluid dynamics software added the subroutines of air drag, electric force, and Coulomb repulsive force on a Lagrangian two-phase flow was used.

1) The multiple-dot lines of charged ink particles that inclined and flew within the electric field of the deflection electrodes were well simulated.

2) The effects of air drag on print distortion were to narrower the first and second lines and curve the lines. The print distortion caused by Coulomb force shows reflects the lower speed of the seventh (top) dot, the wider interval between the sixth- and seventh dots, and the deceleration of the last particle

3) Insertion of dummy particles was shown to make the curved lines of dots straight and parallel.

4) The developed simulation can be used to design CIJPs with fine print quality in computers.

References

[1] W. Thomson (Lord Kelvin), "Receiving or Recording Instruments for Electric Telegraphs," G.B. Patent 2147 (1867).

[2] R. Sweet, "Fluid Droplet Recorder," U.S. Patent 3,596,275 (1963).

[3] C.H. Hertz, and S.I. Simonsson, "Ink-jet Recorder," U.S. Patent 3,416,153 (1966).

[4] S. Matsumoto, T. Inoue, J. Matsuno, and K. Sano, "Flight Stability of Droplets in an Electrostatic Ink-Jet Printer," Trans. of Japan Society of Mech. Eng. (C), 62, (596), pg.1467 (1996).

[5] M. Okano, T. Inoue, Y. Takizawa, T. Matsuda, and A. Miyao, "A New Nozzle for Continuous Inkjet Printers," J. Advanced Mech. Design, Systems, and Manuf., 4, (4), pg.764 (2010).

[6] L. Rayleigh, "On the Instability of Jets," Proc. London Math. Soc. 10, pg.4 (1878).

[7] C. Weber, "Zum Zerfall eines Flussigkeitsstrahles," Z. Angew. Math. Mech. 11, pg.136 (1931).

[8] S. Desai, and M. Lovell, "Computational fluid Dynamics Analysis of a Direct Write Manufacturing Process," Int. J. Nanomanufacturing, 3(3), pg.171 (2009).

[9] M. Ishikawa, E. Ishii, and M. Ikegawa, "Simulation of Gas-Liquid Free Surface Flows in a Refrigerant Distributor and a Nozzle of Continuous-Inkjet," Proc. the ASME IMECE2013, No.63955 (2013).

[10] M. Suzuki, and K. Asano, "A Mathematical Model of Droplet Charging in Ink-jet Printers," J. Phys. D: Appl. Phys., 12, pg.529(1979).

[11] G.L. Filmore, W.L. Buehner, and D.L. West, "Drop Charging and Deflection in an Electrostatic Ink Jet Printer," IBM J. Res. Develop.,21, pg.37 (1997).

[12] M. Ikegawa, and H. Azuma, "Droplet Behaviors on Substrates in Thin Film Formation Using Ink-jet Printing," JSME INT. JOURNAL SERIES B; 47(3), pg. 490 (2004).

[13] H.C. Lee, "Boundary Layer around a Liquid Jet," IBM J. Res. Develop., 21, pg.48(1977).

[14] F. Hendriks, "Aerodynamics of Ink Jet Printing," J. of Applied Photographic Engineering, 6(3), pg.83 (1980).

[15] K. Watanabe, F. Che, and M. Muto, "Study on Coalescence of Droplets of an Ink Jet," Trans. of Japan Soc. of Mech. Eng. (B), 64(619), pg.754(1998).

[16] M. Ikegawa, E. Ishii, N. Harada, and T. Takagishi, "Development of Ink-Particle Flight Simulation for Continuous Inkjet Printer," Proc. the ASME IMECE2013, No.63094 (2013).

[17] STAR-CD, CD-adapco, http://www.cd-adapco.com.

[18] K.V. Beard, and H.R. Pruppacher, "A Determination of the Terminal Velocity and Drag of a Small Water Drops by Means of a Wind Tunnel," J. of the Atmospheric Sciences, 26, pg.1066 (1969).

[19] Y. Tsuji, Y. Morikawa, and K. Terashima, "Fluid-Dynamic Interaction between Two Spheres," Int. J. Multiphase Flow, 8(1), pg.71(1982).

[20] C. Zhu, S.-C. Liang, and L.-S. Fan, "Particle Wake Effects on the Drag Force of an Interactive Particle," Int. Multiphase Flow, 20(1) pg.117 (1994).

Author Biography

Masato Ikegawa received B.E. and M.E. degrees in aeronautics from Tokyo University in 1974 and 1976, respectively. In 1976, he joined Hitachi's Mechanical Engineering Research Laboratory, Japan, where he researched and developed scroll compressors, and numerical simulations such as rarefied gas flow for low-pressure process reactors, LSI process, plasma, HDD airflow, and inkjet. He received a doctor of engineering degree from Tokyo University in 1990. Dr. Ikegawa is a fellow member of the Japan Society of Mechanical Engineers and the Japan Society of Fluid Mechanics and was on their boards of directors (2010-2011).